Design, laser direct writing prototyping, and characterization of fan-out diffractive optical elements for optical interconnect applications

Kyriazis, Athanasios; Vanmol, Koen; Belay, Gebirie Yizengaw; Thienpont, Hugo; Van Erps, Jürgen

Published in:
Design, laser direct writing prototyping, and characterization of fan-out diffractive optical elements for optical interconnect applications

DOI:
10.1117/12.2620785

Publication date:
2022

Document Version:
Submitted manuscript

Design, laser direct writing prototyping, and characterization of fan-out diffractive optical elements for optical interconnect applications

Kyriazis A.[a], Vanmol K.[a], Belay G. Y.[a], Thienpont H.[a], and Van Erps J.[a]

[a]Brussels Photonics (B-PHOT), Dept. Of Applied Physics and Photonics, Vrije Universiteit Brussel and Flanders Make, Pleinlaan 2, B-1050 Brussel, Belgium

ABSTRACT

We present the design, fabrication, and characterization cycle of a diffractive optical element based layout, used for 1-to-7 power splitting of a Gaussian beam emitted by a single-mode fiber. First, a modified version of our earlier demonstrated mode conversion up-taper structure is designed, fabricated, and characterized, increasing the mode-field diameter of the fundamental mode by a factor of 2. Then, a newly designed diffractive optical element is optimized to convert the expanded field distribution to a seven Gaussian-spot hexagonal array with 45 μm spacing, at an optimal propagation distance of only 61 μm, achieving splitting in a non-paraxial diffraction regime. The two components are combined into a monolithic design encompassing both adiabatic field expansion and efficient phase modulation in a single, highly miniaturized component. The power splitter is fabricated directly on the cleaved facet of a single-mode fiber, in a single step, using direct laser writing based on two-photon polymerization. The small spatial extent of the power splitter allows for a highly compact, integrated solution for wide-angle, fan-out power splitting of a Gaussian beam in single-mode interconnect and sensing applications.

Keywords: Two-photon polymerization, diffractive optical element, direct laser writing, fiber beam splitter, monolithic integration

1. INTRODUCTION

Microfabrication using two-photon polymerization (2PP)-based direct laser writing (DLW) has recently evolved into a research standard for the realization of optical micro-components, such as fiber micro-connectors [1], light-couplers [2], pre-aligned micro-lenses [3], and planar waveguides [4]. In addition, the idea of using DLW to create nano-structures directly on the fiber facet has also been in the foreground for quite some time. Since the work of Liberale et al. in 2010 [5], the assets of DLW have made it a preferred technique for fiber-tip fabrication in a variety of applications. During the last decade, DLW on fiber tips has extensively been employed to create, among others, anti-reflective coatings [6], beam shaping phase masks [7] and free-form coupling elements [8]. Furthermore, coupling via lens arrays printed directly on a multi-core fiber facet for use in astronomy instrumentation [9], and a polarizing beam splitter using a 3D-printed prism and a sub-wavelength Lamellar grating have been demonstrated [10].

Evidently, direct laser writing on the fiber tip has become the enabling technology in domains where optical fibers are employed, such as optical communications and sensing applications. In optical interconnects, the ever growing trend in the volume of transferred information and network speeds impose high demands for reliable, but also versatile connections. The signal often needs to be split into different communication lines, amplified, recombined and in general, modulated. Within the optical fiber sensing domain, acquiring local measurements of fluctuating environmental parameters with minimal impact is required. Therefore, splitting the optical signal from a single-mode fiber (SMF) to multiple detection points would allow for scalable solutions for extrinsic fiber sensors.

Further author information: (Send correspondence to A.K.)
A.K. E-mail: Athanasios.Kyriazis@UGent.be

One flexible way to achieve these types of wavefront manipulation is by integrating diffractive structures on the fiber tip using various micro-fabrication techniques [11–13]. However, the beam modulating capability of the diffractive optical elements (DOE) is restricted by the limited illuminated area of the SMF mode-field (with a typical diameter of 10 μm). A solution is to expand the mode-field diameter (MFD) by letting the beam propagate in a homogeneous medium before it impinges on the DOE, e.g., by using a polymer cylinder [14]. However, in this type of approaches, the fundamental mode is diffracted into the bulk of the optical medium, which may lead to distortion of the intensity profile. Therefore, a preferred strategy is to use tailor-made mode-field conversion elements to ensure MFD increase or decrease, in a controlled, profile-preserving way [15, 16]. Of special interest to us is the previous work of Vanmol et al. [17], where a micro-structured up-taper for threefold adiabatic expansion of the SMF mode-field area is 3D-printed on the fiber facet. Nevertheless, combining the aforementioned different components for both beam expansion, as well as wavefront modulation is not straightforward, especially if the fabrication techniques are not compatible.

In this work we exploit the freedom of 2PP-DLW, to demonstrate the combined functionality of a DOE-based fiber beam splitter in a compact implementation. We first elaborate on the design and optimization of a DOE for 1-to-7 power-splitting of a standard SMF mode-field. Parallelly, we present a modified, enhanced design of the microstructured optical fiber (MOF) up-taper demonstrated in [17]. Next, we bring together the DOE with the MOF up-taper in a single 3D-model, and demonstrate the fabrication of the whole monolithic structure on the fiber facet, in a single fabrication step. Finally, the fiber-beam splitter is characterized with respect to its wide-angle beam splitting capability.

2. DESIGN OF THE DIFFRACTIVE OPTICAL ELEMENT

A DOE design starts with the definition of the source field (input) and the desired output field. The functionality of the DOE is to transform the input field into the desired distribution over a predefined propagation distance (PD). In this work, the input field is defined as an expanded Gaussian beam with an MFD ($1/e^2$) of 20 μm. The output field consists of 7 Gaussian beams with a full-width at half-maximum (FWHM) of 11.5 μm, spaced apart by 45 μm in a hexagonal layout, formed at a PD of 61 μm (Fig. 1). The spot-pitch along with the short PD result in a targeted splitting angle of approximately 72°, for two diametrically opposite spot centers. To minimize the energy losses, we design the DOE so that no part of the input field is blocked. This is often called a *phase-only design*, indicating that diffraction is exploited by modulating only the phase of the source field distribution at each point, $\Delta\varphi(x, y)$. To calculate the phase change profile, we use the Iterative Fourier Transform Algorithm (IFTA), also known as *error-reduction* or *Gerchberg & Saxton* algorithm [18]. The used simulation software providing the framework for the IFTA-based DOE design was VirtualLab Fusion by LightTrans [19].

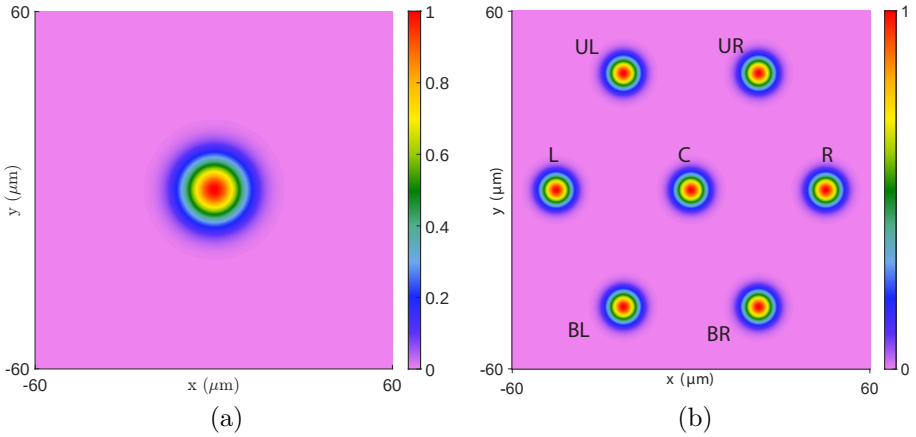

Figure 1: The basic fields used by the IFTA. The color mapping represents the normalized amplitude. (a) The input field, approximated by a Gaussian beam with a 10 μm radius. (b) The desired output field, approximated by seven 11.5 μm-FWHM Gaussian beams, fixed to a hexagonal layout of 45 μm pitch. The capital letters are used for spot indexing.

Regarding the DOE geometry, we can conceptually divide the specifications in the vertical (out-of-plane) and the lateral (in-plane) direction. Vertically, i.e. along the propagation direction, although the IFTA inherently yields a continuous solution for the phase distribution, an 8-level quantization is performed. More levels would exceed the fabrication capabilities, whereas fewer would compromise the performance of the DOE. On the other hand, the lateral DOE design is determined by its pixel size (or sampling distance l_{px}), the number of sampling points (pixels) in one direction (N) and its size (d); the diameter of a circular DOE (see Fig. 2). These parameters are coupled: $d = N \cdot l_{px}$. The lateral resolution of the DOE was set to 200 nm to match the smallest feature size the DLW printer can achieve. The DOE diameter is fixed at 34 μm, which is almost twice the source MFD (a practice usually followed to ensure all incident light is effectively exploited). The specifications of the DOE are summarized in Table 1.

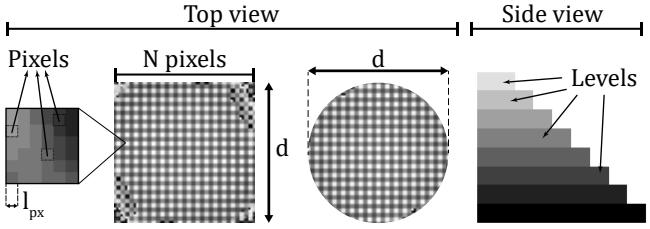

Figure 2: An illustration of the basic geometrical characteristics of a DOE: pixel size (l_{px}), number of sampling points (N), and its size (d) are depicted in the top view. The DOE levels are shown in the side view. The grayscale color mapping is used to indicate height variability, as lighter tones represent higher levels.

Table 1: Geometrical and functional specifications for the IFTA-based DOE design.

Basic DOE Specifications	
Quantization	8 levels
Modulation type	Phase-only
Wavelength λ (μm)	1.55
Diameter (μm)	34
Sampling distance (μm)	0.2×0.2
Propagation distance (μm)	61

The output field simulated with the IFTA-based solution exhibits a non-uniform intensity distribution (a brighter central spot), and elongated outer spots (Fig. 3-a). The elongation direction is calculated for each individual spot and is consistently found to be radial. To counteract these problems, the IFTA execution was optimized by modifying the desired output field. More specifically, the central spot brightness was reduced, and the outer spot circular intensity contour shape was replaced by ellipses with the minor axis radially aligned. The result is the optimized simulated output field, seen in Fig. 3-b. The elongation is reduced from 21.3 % to 14.9 %, and the relative standard deviation of the peak spot intensity is minimized (from 13.4 % to 0.6 %). To estimate the losses of the splitter, the conversion efficiency (CE) of the optimized design is calculated ($\approx$ 73.4 %).

3. FABRICATION

The current printer system requires 3D-representations of the elements to be manufactured. For the MFD expansion up-taper, the already existent model presented in [17] was modified. Firstly, after the appropriate simulations, the taper length was increased to expand the MFD even further than the demonstrated MFD of $\approx$ 17 μm, to match the simulated DOE input MFD $\approx$ 20 μm. In addition, for efficient integration with the DOE, extra side-channels were added, aiding the photoresist development step in the fabrication process. On the other hand, to create a 3D-model for the optimized phase profile, the height of the DOE at each point is proportionally

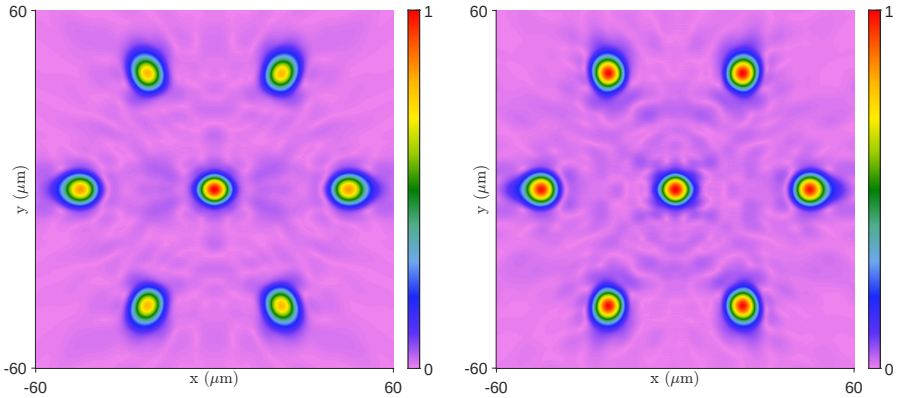

Figure 3: Normalized intensity amplitude distribution of the simulated output fields, before and after optimization. (a) The output field of the IFTA-based DOE solution. (b) The output field after the final shape and uniformity optimization.

associated with the phase difference according to the relationship:

$$\mathrm{d(x,y)} = \frac{\Delta\varphi(\mathrm{x,y})}{2\pi}\frac{\lambda}{(\mathrm{n_1}-\mathrm{n_0})} \tag{1}$$

where $\mathrm{d(x,y)}$ is the *modulation depth*, $\Delta\varphi(\mathrm{x,y})$ is the relative phase difference, λ is the wavelength of the incident light, and $\mathrm{n_1}, \mathrm{n_0}$ are the refractive indices (RI) of the DOE material and the surrounding medium, respectively [20]. The result is a DOE with a maximum height $\mathrm{d_{max}} \approx 2.55$ μm, and each level separated by a level height $\delta = 364$ nm (see also Fig. 4).

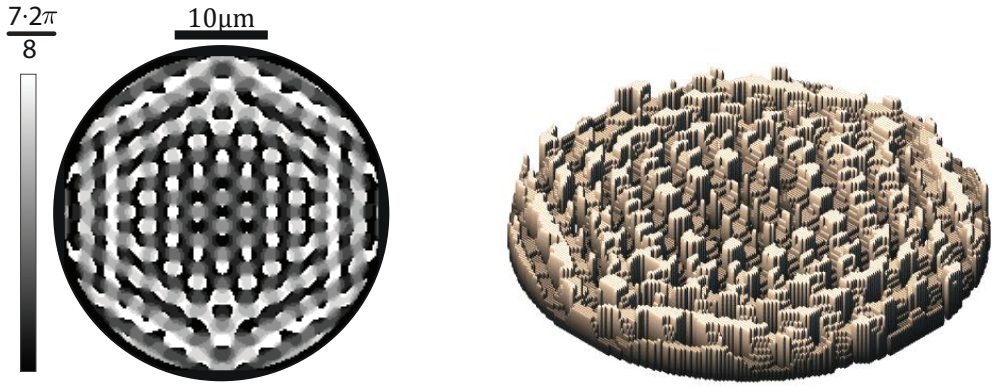

Figure 4: Optimized 8-level DOE. The diameter is 34 μm and the maximum height is ≈ 2.55 μm. (a) Bitmap representation. The grayscale color mapping represents the phase in radians. (b) Isometric view of the 3D-model rendered in Nanoscribe's software (Describe).

The fiber beam splitter components were 3D-printed using the Photonic Professional GT+ system, and selecting the IP-Dip as a photoresist, both commercially available from the company Nanoscribe [21]. The laser source is a pulsed femtosecond fiber laser, centered around the near infra-red (IR) wavelength of 780 nm, and it is focused into the negative-tone photoresist by a high numerical aperture (NA) objective lens. The fabrication process starts with a cleaved fiber, firmly clamped by a V-groove-like assembly. An IP-Dip droplet is dropcasted, immersing the fiber facet, and the holder is placed on the printer's piezo-electric translation stage. For our

purposes, the objective lens was immersed in the photoresist volume, in what is commonly referred to as dip-in laser lithography (DiLL) configuration. After the alignment and the fabrication, the sample is developed in Propylene glycol methyl ether acetate (PGMEA) for about 20 min, and then rinsed by submerging into isopropyl alcohol (IPA) for less than 5 min.

The modified up-taper was first fabricated on the fiber tip and subsequently characterized (see section 4). After validating the expected performance, the up-taper and the DOE were combined into a monolithic model which allowed for a single-step fabrication. The fabricated splitter is shown in Fig. 5. It is worth noting that highly localized spatial content has been accurately fabricated (e.g. the high aspect-ratio peaks near the center of the DOE).

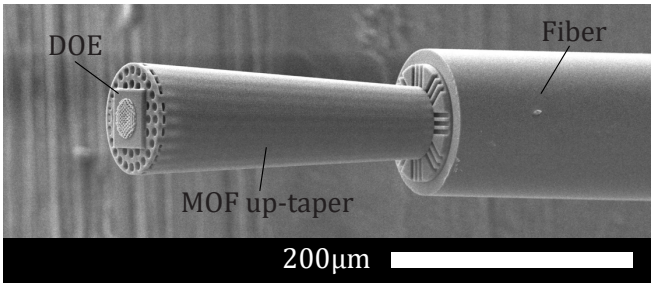

(a)

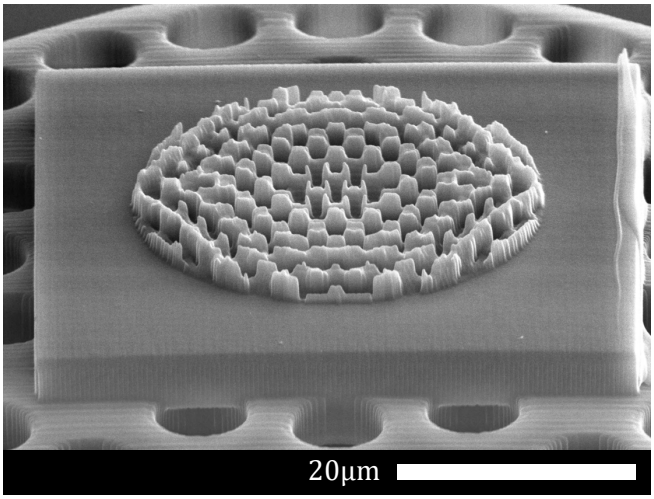

(b)

Figure 5: Scanning-electron microscope (SEM) images of the fiber beam splitter, fabricated using 2PP. (a) The MOF up-taper is fabricated on the fiber facet, and the DOE is fabricated on top of it. (b) A close-up of the DOE. The square base is a byproduct of discrete-type 3D-model processing of the printing software.

4. CHARACTERIZATION

As we already mentioned, an important step was to measure the output field at the up-taper facet, to ensure that the DOE would have the correct input MFD. Since the operation wavelength is 1550 nm, the fiber was connected to the respective laser source. To observe the output, we used a Bobcat IR camera by Xenics, along with 20×–NA 0.5 and 50×–NA 0.6 microscope objectives by SEIWA. Two fabricated up-tapers were measured and the MFD was found to be 22.0 μm, with the measurement uncertainty being approximately 1.1 μm, confirming the intended up-taper functionality. The up-taper and its output field can be seen in Fig. 6.

To optically characterize the whole fiber beam splitter, the previous configuration is not suitable. The limited NA of the objective lens is not sufficient to capture the split beam components which form a wide angle with

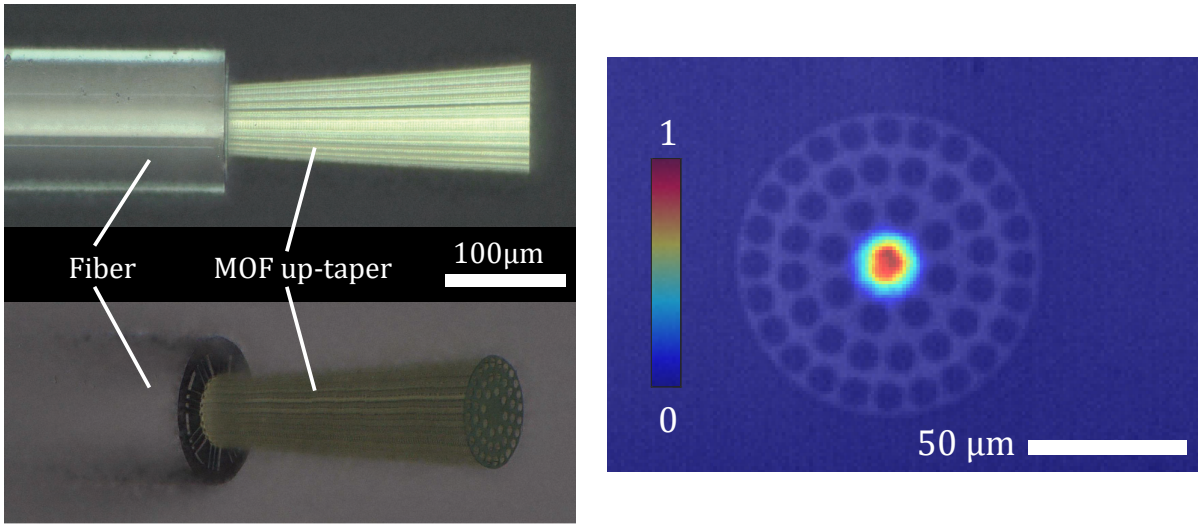

(a) (b)

Figure 6: (a) Optical microscope images of the MOF up-taper printed on top of a single-mode fiber facet. The side view is shown at the top, whereas at the bottom, a perspective view shows the side-channels near the base and the facet of the up-taper. (b) The MOF up-taper facet and the respective output field in overlay. The color-bar depicts the normalized intensity.

respect to the optical axis ($\approx 36°$). Using an objective with a higher NA limits the field-of-view significantly, which—along with the positioning limitations—makes the observation extremely difficult. Therefore, the characterization is performed by directly projecting the output field to the sensor placed a few millimeters away from the splitter, without interposing any lenses (see Fig. 7-a). The central core is substantially brighter, but the outer spots are clearly evident.

To estimate the deviation angle, we started from the initial position where the field was captured ($\Delta z = 0$), and we gradually increased the distance between the sensor and the splitter. At each point, we acquired the intensity distribution and we graphically measured the distance from the central spot to each of the outer ones; i.e. 6 lateral distance values Λ_{S_i}, one for each outer spot ($i = UL, UR, BL, BR, L, R$), at a specific Δz position. These 6 values were averaged to estimate a representative inter-spot distance (spot-pitch) Λ_S for each Δz. The spot-pitch (Λ_S) was plotted against the relative splitter-sensor distance (Δz) and a linear regression was performed (Fig. 7-b). The slope of the regression line reveals the deviation angle: $\arctan(0.7185) \approx 36°$.

The match with the designed value indicates that the designed desired pattern with a spot-pitch of 45 μm should be present at the designed propagation distance of 61 μm, although it was not directly imaged. On the other hand, making such an extrapolation for dimensions which are a few orders of magnitude smaller than our observation scale, should be handled with caution. At the μm-scale, near-field diffraction effects might occur which are not present in longer distances and are thus not apparent in our macro-scale observations. As a final indication, the Fresnel number was calculated for our diffractive system. More specifically, for beam diffraction through a slit (or an aperture), the Fresnel number is defined as $N_F = a^2/(L\lambda)$, where a is the slit width (or aperture diameter), L is the propagation distance, and λ is the wavelength of the beam. If $N_F \ll 1$, the system operates in the far-field, i.e. near-field effects have attenuated. In our calculations, using $a = 200$ nm (the DOE lateral feature size) as the slit width, $L = 61$ μm, and $\lambda = 1.55$ μm, satisfies the $N_F \ll 1$ criterion. Consequently, this indicates that the diffraction at 61 μm and at mm-scale, both exist under the far-field diffraction regime and our trust in our extrapolation validity is strengthened. Precise measurement of the output field at 61 μm is the subject of future work.

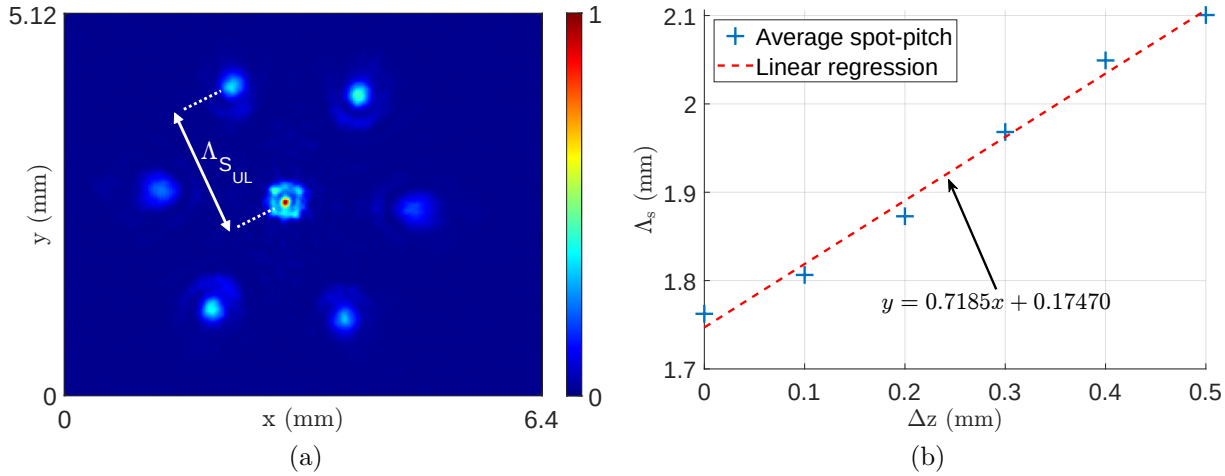

Figure 7: (a) The fiber beam splitter output field intensity, captured directly by the sensor. Note the bright central region due to undiffracted light. The arrow depicts the distance from the central spot to the UL core $\Lambda_{S_{UL}}$. (b) The average distance between the central spot and the outer spots (Λ_S) at various propagation distances. Δz denotes the relative displacement along the propagation direction (z-axis), with respect to an initial positioning distance between the splitter and the sensor. Λ_S is graphically estimated from the acquired intensity fields. The slope of the linear regression reveals the diffraction angle of the outer split beam components (36°).

5. CONCLUSION

In this work, we designed, fabricated and characterized a 1-to-7 power-splitting DOE-based structure using 2PP-based DLW. The DOE has a circular-footprint diameter of 34 μm, comprises 8 discrete equidistant height levels with a total height of 2.55 μm, operating at a wavelength of 1550 nm. It is designed to modulate a Gaussian beam with an MFD of 20 μm as an input, to yield a hexagonal 45 μm spot-pitch, 7-spot output at a full pattern diffraction angle of 72°. The DOE was fabricated on the facet of a beam expanding up-taper structure, inspired by the design of microstructured optical fibers (MOF up-taper). The latter was 2PP-printed on top of a standard SMF facet. The expanded mode-field was measured, and the MFD was found to be 22 μm with a measurement uncertainty of 1.1 μm.

Using 2PP-based DLW, a monolithic design consisting of the MOF up-taper and the DOE was printed on the fiber facet, in a single fabrication step. The total height of the beam splitter is 295 μm. Measurements at mm-scale propagation distance revealed the deviation angle to be equal to the designed $\approx 36°$. Power splitting in such wide angles can be beneficial for use-cases where non-paraxial diffraction patterning is required, such as closely-spaced detectors at small propagation distances, allowing for sensor footprint reduction and form-factor improvement in optical interconnect and fiber sensing applications.

ACKNOWLEDGMENTS

This work was financially supported by Interreg (NWE758, Fotonica Pilootlijnen); Fonds Wetenschappelijk Onderzoek (G020621N, I013918N); Flanders Make; Belgian Federal Science Policy Office; Herculesstichting (Hercules/FWO UAB/13/10); Methusalem foundation; Industrial Research Fund (IOF) and OZR of the Vrije Universiteit Brussel.

REFERENCES

[1] Bogucki, A., Zinkiewicz, Ł., Pacuski, W., Wasylczyk, P., and Kossacki, P., "Optical fiber micro-connector with nanometer positioning precision for rapid prototyping of photonic devices," *Opt. Express* **26**, 11513–11518 (4 2018).

[2] Pisarenko, A., Zvagelsky, R., Kolymagin, D., Katanchiev, B., Vitukhnovsky, A., and Chubich, D., "DLW-printed optical fiber micro-connector kit for effective light coupling in optical prototyping," *Optik* **201**, 163350 (2020).

[3] Thiele, S., Pruss, C., Herkommer, A. M., and Giessen, H., "3D printed stacked diffractive microlenses," *Opt. Express* **27**, 35621–35630 (11 2019).

[4] Baghdasaryan, T., Vanmol, K., Thienpont, H., Berghmans, F., Geernaert, T., and Erps, J. V., "Design and two-photon direct laser writing of low-loss waveguides, tapers and S-bends," *Journal of Physics: Photonics* **3**, 045001 (8 2021).

[5] Liberale, C., Cojoc, G., Candeloro, P., Das, G., Gentile, F., De Angelis, F., and Di Fabrizio, E., "Micro-optics fabrication on top of optical fibers using two-photon lithography," *IEEE Photonics Technology Letters* **22**(7), 474–476 (2010).

[6] Kowalczyk, M., Haberko, J., and Wasylczyk, P., "Microstructured gradient-index antireflective coating fabricated on a fiber tip with direct laser writing," *Opt. Express* **22**, 12545–12550 (5 2014).

[7] Gissibl, T., Schmid, M., and Giessen, H., "Spatial beam intensity shaping using phase masks on single-mode optical fibers fabricated by femtosecond direct laser writing," *Optica* **3**, 448–451 (4 2016).

[8] Dietrich, P.-I., Blaicher, M., Reuter, I., Billah, M., Hoose, T., Hofmann, A., Caer, C., Dangel, R., Offrein, B., Troppenz, U., Freude, W., and Koos, C., "In-situ 3D nano-printing of freeform coupling elements for hybrid photonic integration," *Nature Photonics* **12** (04 2018).

[9] Dietrich, P.-I., Harris, R. J., Blaicher, M., Corrigan, M. K., Morris, T. J., Freude, W., Quirrenbach, A., and Koos, C., "Printed freeform lens arrays on multi-core fibers for highly efficient coupling in astrophotonic systems," *Opt. Express* **25**, 18288–18295 (7 2017).

[10] Hahn, V., Kalt, S., Sridharan, G. M., Wegener, M., and Bhattacharya, S., "Polarizing beam splitter integrated onto an optical fiber facet," *Opt. Express* **26**, 33148–33157 (12 2018).

[11] Prasciolu, M., Cojoc, D., Cabrini, S., Businaro, L., Candeloro, P., Tormen, M., Kumar, R., Liberale, C., Degiorgio, V., Gerardino, A., Gigli, G., Pisignano, D., Di Fabrizio, E., and Cingolani, R., "Design and fabrication of on-fiber diffractive elements for fiber-waveguide coupling by means of e-beam lithography," *Microelectronic Engineering* **67-68**, 169 – 174 (2003). Proceedings of the 28th International Conference on Micro- and Nano-Engineering.

[12] Vanek, M., Vanis, J., Baravets, Y., Todorov, F., Ctyroky, J., and Honzatko, P., "High-power fiber laser with a polarizing diffraction grating milled on the facet of an optical fiber," *Opt. Express* **24**, 30225–30233 (12 2016).

[13] Calafiore, G., Koshelev, A., Allen, F. I., Dhuey, S., Sassolini, S., Wong, E., Lum, P., Munechika, K., and Cabrini, S., "Nanoimprint of a 3D structure on an optical fiber for light wavefront manipulation," *Nanotechnology* **27**, 375301 (8 2016).

[14] Schmidt, S., Thiele, S., Toulouse, A., Bösel, C., Tiess, T., Herkommer, A., Gross, H., and Giessen, H., "Tailored micro-optical freeform holograms for integrated complex beam shaping," *Optica* **7**, 1279–1286 (10 2020).

[15] Vanmol, K., Tuccio, S., Panapakkam, V., Thienpont, H., Watté, J., and Van Erps, J., "Two-photon direct laser writing of beam expansion tapers on single-mode optical fibers," *Optics & Laser Technology* **112**, 292 – 298 (2019).

[16] Vanmol, K., Saurav, K., Panapakkam, V., Thienpont, H., Vermeulen, N., Watté, J., and Van Erps, J., "Mode-field matching down-tapers on single-mode optical fibers for edge coupling towards generic photonic integrated circuit platforms," *Journal of Lightwave Technology* **38**(17), 4834–4842 (2020).

[17] Vanmol, K., Baghdasaryan, T., Vermeulen, N., Saurav, K., Watté, J., Thienpont, H., and Erps, J. V., "3D direct laser writing of microstructured optical fiber tapers on single-mode fibers for mode-field conversion," *Opt. Express* **28**, 36147–36158 (11 2020).

[18] Gerchber, R. W. and Saxton, W. O., "A practical algorithm for the determination of phase from image and diffraction plane pictures," *OPTIK* **35**(2), 237–246 (1972).

[19] "VirtualLab Fusion: Optical Design Software from LightTrans." https://www.lighttrans.com/. Online; Accessed: 2021-04.

[20] O'Shea, D. C., Suleski, T. J., Kathman, A. D., and Prather, D. W., [*Diffractive Optics: Design, Fabrication, and Test*], SPIE PRESS, Bellingham, Washington USA (2003).

[21] "Photonic Professional GT2: Nanoscribe." https://www.nanoscribe.com/en/products/photonic-professional-gt2. Online; Accessed: 2021-05-01.